03,11

# Structural transformation of $\alpha$- and $\kappa$-$Ga_2O_3$ thin films on sapphire upon annealing in air

© A.V. Myasoedov[1], I.S. Pavlov[2], M.P. Scheglov[1], A.I. Pechnikov[1], V.I. Nikolaev[1]

[1] Ioffe Institute,
St. Petersburg, Russia
[2] Federal Research Center „Crystallography and Photonics“ RAS,
Moscow, Russia

E-mail: amyasoedov88@gmail.com

*Received August 1, 2023*
*Revised August 1, 2023*
*Accepted August 3, 2023*

The results of a study of the effect of annealing on the structural transformation of thin films of $\alpha$- and $\kappa$-$Ga_2O_3$ obtained by chloride vapor-phase epitaxy on $c$-plane of a sapphire substrate are presented. It has been shown that upon annealing of an $\alpha$-$Ga_2O_3$ film during 60 min at a temperature in the region of the polymorphic transition of 550−575°C, its homogeneity begins to be disrupted, and a partial polymorphic transition is observed with the formation of small $\beta$-$Ga_2O_3$ crystallites. As a result of high-temperature annealing of the $\kappa$-$Ga_2O_3$ film in air for 30 min at a temperature $T = 850°C$, the $\kappa \to \beta$ transition and recrystallization of the original film into a homogeneous $\beta$-$Ga_2O_3$ film were observed. It was found that the resulting film predominantly consists of mutually oriented domains. Using transmission electron microscopy, the orientation relationships between the film and the sapphire substrate were determined. The structure of boundaries between domains has been studied.

**Keywords:** gallium oxide, polymorphism, polymorphic transitions.

DOI: 10.61011/PSS.2023.10.57215.172

## 1. Introduction

Gallium oxide ($Ga_2O_3$) is ultrawide bandgap semiconductor material promising for applications as solar-blind UV photodetectors [1], high voltage field-effect transistors [2], Schottky diodes [3] and gas sensors [4]. In addition to the thermally stable $\beta$-phase, the increasing interest is being paid to metastable modifications: $\alpha$, $\gamma$, $\kappa$ and $\delta$ having some significant advantages [5], so $\alpha$-$Ga_2O_3$ with corundum structure has values of band gap $E_g = 5.3$ eV [6] and more high hardness [7] that are largest among others polymorphs. Orthorhombic $\kappa$-$Ga_2O_3$ is second phase in terms of stability after monoclinic $\beta$-$Ga_2O_3$. High values of spontaneous polarization along the direction $c$ [8,9] were predicted for it, this is promising from the point of view of creating high electron mobility transistors. Mostly, $\alpha$ and $\kappa$-$Ga_2O_3$ are obtained as form of thin films by heteroepitaxy, as a rule on sapphire substrates [10–12]. Due to the fact that with temperature increasing the polymorphic transformations take place in metastable phases and, ultimately, a transition to $\beta$-$Ga_2O_3$, special attention is directed to study ways to increase thermal stability of metastable polymorphs [13–17].

The Table presents the structural data of films of the three main polymorphs of gallium oxide. It is believed that temperature of beginning of polymorphic transformations of $\alpha$-$Ga_2O_3$ is significantly below the same of $\kappa$-$Ga_2O_3$ [16,18]. The paper [13] states that the $\alpha$-phase remained stable only up to 550°C, then it gradually transforms into the $\beta$-phase. The presented X-ray diffraction patterns of $\alpha$-$Ga_2O_3$ film during the annealing show how with temperature increasing the decrease in the 0006 reflection peak is observed, and the a broad peak in the region of $\bar{4}02$ reflection for $\beta$-$Ga_2O_3$ appears. This indicates that the film undergoes polymorphic transformation into the $\beta$-phase, at that small crystallites are formed, they are oriented with respect to the sapphire substrate close to the position $(\bar{2}01)_\beta \parallel (0001)_{\text{sapphire}}$. For polymorphic transition of $\kappa$-$Ga_2O_3$ to high temperature phase the temperatures in more wide range 650−1000° C are given [14–16,19]. At this for $\kappa$-$Ga_2O_3$ the transition to structure $\beta$-$Ga_2O_3$ is observed, its crystallites are coupled with sapphire substrate by relationship $(\bar{3}10)_\beta \parallel (0001)_{\text{sapphire}}$. It is worth noting individually that X-ray diffraction studies of the polymorphic transition $\kappa \to \beta$ require special attention, when analyzing reflections 002, 004, 006 and 008 typical for $\kappa$-$Ga_2O_3$ film with orientation (001), because their position is very close to the reflections $\bar{2}01$, $\bar{4}02$, $\bar{6}03$ and $\bar{8}04$ for $\beta$-$Ga_2O_3$ with orientation $(\bar{2}01)$. This circumstance will be explained in more detail during results discussion.

During polymorphous transition between gallium oxide phases the rearrangement of the crystal structure and change in the physical properties of the crystal occur. Comparison of density values for these three structures (see Table) shows that the polymorphous transition $\alpha \to \beta$ shall be accompanied by a significant increase in the specific volume of the film. For clarity, the Table shows volume values normalized to 20 atoms — 8 atoms of gallium and 12 atoms of oxygen. Thus, the change in volume during the transition from the metastable $\alpha$- to the stable $\beta$-phase is $\sim 9\%$.

Structural properties of gallium oxide polymorphs

| Phase | Syngony | Group | $N_{atom}$ | $V_{cell}$, Å$^3$ | $V(8+12)$, Å$^3$ | $\rho_{calc}$, g · cm$^{-3}$ | $\rho_{exp}$, g · cm$^{-3}$ |
|---|---|---|---|---|---|---|---|
| $\alpha$-$Ga_2O_3$ | Rhombohedral | $R\bar{3}c$ | $12+18$ | 288.8 [21] | 192.5 | 6.46 | 6.48 [22] |
| $\beta$-$Ga_2O_3$ | Monoclin. | $C2/m$ | $8+12$ | 208.9 [23] | 208.9 | 5.96 | 5.94 [22] |
| $\kappa$-$Ga_2O_3$ | Orthorhomb. | $Pna2_1$ | $16+24$ | 423.6 [24] | 211.8 | 5.88 | 5.94 |

Already during annealing for 5 min at temperature of 600°C, an irreversible process of degradation begins, accompanied by its cracking [17]. At the same time, the difference in the change in specific volume during the transition from $\kappa$-phase to $\beta$-phase turns out to be insignificant. It was noted in the paper [15] that the film transition can occur either with or without its cracking, depending on the annealing parameters. The Table shows the density values calculated based on the number of atoms per volume of one unit cell — $\rho_{calc}$ and experimentally measured $\rho_{exp}$. The initial films of the $\kappa$-phase are polycrystalline [20] with many vertical grain boundaries. The experimental results in the Table are given based on the data available in the publications and the results of experimental measurements by the method of hydrostatic weighing of density of the separated from substrate thick layer of $\kappa$-phase.

## 2. Experimental methods

Thin films $Ga_2O_3$ were obtained by chloride vapor-phase epitaxy on sapphire substrates with an orientation (0001). The synthesis was carried out at atmospheric pressure in a horizontal quartz reactor developed in LLC „Perfect Crystals" [25] at 500°C ($\alpha$-$Ga_2O_3$) and 550°C ($\kappa$-$Ga_2O_3$). The growth rate varied from 8 to 12 $\mu$m · h$^{-1}$. For study several samples with layers thickness of 0.8 to 1.8 $\mu$m were selected. The obtained during growth films $\alpha$-$Ga_2O_3$ had mirror-like surface. The phase composition of the films was determined by X-ray diffraction analysis; it was carried out before and after each annealing. The surface morphology and structure of film were studied by scanning electron microscopy (SEM) and transmission electron microscopy (TEM), respectively.

TEM-studies were carried out on an electron microscope Tecnai Osiris (FEI Technologies Inc.) at an accelerating voltage of 200 kV. Film cross sections were prepared using a focused ion beam $Ga^+$on Scios FEI FIB setup in form of lamella. SEM-studies were also performed using this setup.

## 3. Structure of films $\alpha$-$Ga_2O_3$ after annealing

A study of sample with a $\alpha$-$Ga_2O_3$ film after two-stage annealing for 30 min at 550 and 575°C, respectively, showed that the film transformation occurs non-uniformly over area with the local formation of centers similar to the centers of homogeneous nucleation, which begin to increase their area, forming a specific pattern on the surface. Namely, after two stages of annealing a mesh of triangular-shaped „islands" $\alpha$-$Ga_2O_3$ is observed, separated by regions where degradation of the monocrystalline layer occurred. It is obvious that this pattern of islands is associated with the symmetry of corundum, namely the presence of a three-fold axis. The results of X-ray diffraction analysis of the film after two-stage annealing are shown in Figure 1, *a*. The X-ray pattern clearly shows a set of reflections $\bar{2}01$, $\bar{4}02$, $\bar{6}03$ and $\bar{8}04$, corresponding to $\beta$-$Ga_2O_3$. Peak 0006 (40.2°) of $\alpha$-phase is overlapped with reflection $\bar{4}02$ (38.3°) and 0006 (41.3°) of substrate. The presence of the $\alpha$-phase was unambiguously established from the results of analysis of electron microdiffraction patterns obtained for film cross section in TEM. Thus, the correspondence of areas with smooth surface to $\alpha$-phase was established. Figure 1, *b* shows SEM-image of boundaries of $\alpha$-$Ga_2O_3$ and $\beta$-$Ga_2O_3$ regions. The given photo shows that after temperature degradation the morphology of the film surface changes dramatically. The film with an almost perfectly smooth surface is replaced by a rough film, highly heterogeneous in thickness, with many discontinuities and the absence of a regular crystalline facet. The zoomed up image of the region subjected to phase transformation is shown in Figure 1, *c*. It shows that lamination is observed in the resulting structure of gallium oxide, and discontinuities exposing the substrate were formed in the film. Figure 1, *d* shows TEM-image of film cross-section, cut from the area with a flat surface morphology. Analysis of electron microdiffraction patterns in this region confirmed that the area of film consists of $\alpha$-$Ga_2O_3$ phase without inclusions of other phases. Thickness of studied film was determined as equal to 1.8 $\mu$m.

## 4. Structure of films $\kappa$-$Ga_2O_3$ after annealing

The results of X-ray diffraction analysis of $\kappa$-$Ga_2O_3$ film after high-temperature annealing indicate that polymorphic transition to the $\beta$-phase took place. In Figure 2, *a* X-ray pattern indicates two sets of observed reflections: first, related to $\beta$-$Ga_2O_3$: $\bar{3}\bar{1}0$ (37.1°), $\bar{6}\bar{2}0$ (79.1°) and the second one, which can be attributed to or to 002 (18.9°), 004 (38.2°), 006 (58.8°) $\kappa$-phase, or $\bar{2}01$ (18.9°), $\bar{4}02$ (38.3°), $\bar{6}03$ (58.9°) for $\beta$-$Ga_2O_3$. As

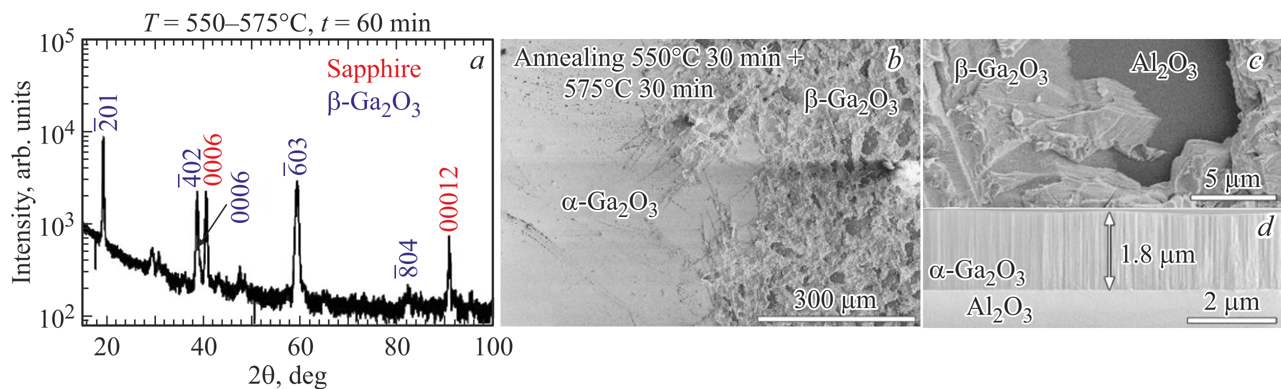


**Figure 1.** Results of study of sample with $\alpha$-$Ga_2O_3$ film after annealing at temperature 550−575°C. *a* — X-ray diffraction pattern of sample; *b* — SEM image of film surface; *c* — zoomed up image of surface section after degradation, discontinuity is observed; *d* — cross-sectional TEM-image of film area keeping its structure.

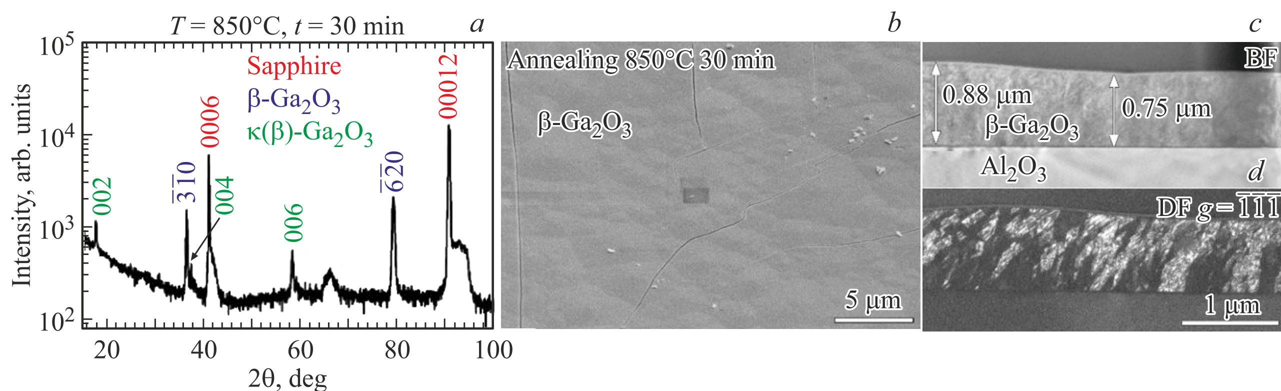


**Figure 2.** Results of studying sample with $\kappa$-$Ga_2O_3$ film after high-temperature annealing. *a* — X-ray diffraction pattern of the sample; *b* — SEM images of surface morphology; *c* — brightfield TEM image of film cross-section; *d* — dark-field TEM image of the same area $\bar{1}\bar{1}\bar{1}$.

stated in the introduction, these sets almost completely duplicate each other. Considering that the calculated intensity values for the first set of reflections are almost by two orders of magnitude lower than for the second one, we can conclude that the orientation $(\bar{3}\bar{1}0)$ is preferable for domains. We attribute the second set of reflections to the residues of the initial phase $\kappa$-$Ga_2O_3$ with orientation (001). This result is partially confirmed by TEM data. Formation of domains $\beta$-$Ga_2O_3$ with orientation $(\bar{2}01)$ after high-temperature annealing was noted in paper [16]. Domains had orientation relationships with substrate similar to films $\beta$-$Ga_2O_3$ obtained on sapphire by heteroepitaxy [1,26,27], — $(\bar{2}01) \parallel (0001)$ and directions $[1\bar{3}2]$, $[\bar{1}\bar{3}\bar{2}]$ and [010], oriented along directions of type $\langle 1\bar{1}00 \rangle$ substrate. Such orientation relationships are determined by the three-fold axis of sapphire. Our TEM-study did not identify $\beta$-$Ga_2O_3$ domains with orientation $(\bar{2}01)$. Also note the results of the paper [14], where *in situ* in vacuum and *ex situ* in air the process of $\kappa \to \beta$ phase transition was studied during annealing of sample prepared for TEM-study. The authors found that during annealing in air at temperatures up to 820°C a partial polymorphic transition $\kappa \to \gamma$ occurs without the start of formation of $\beta$-phase. At higher temperatures in vacuum the transition to $\beta$-phase with the addition of intermediate $\gamma$-phase is observed. Thus, in this temperature range one can expect stabilization of the intermediate $\gamma$-phase. During the TEM-study, we did not detect the presence of the $\gamma$-phase. This can be explained by the fact that TEM sample annealing in air or in vacuum differs from the annealing of bulk films in that the former has different free surfaces, and other mechanical stresses act.

Surface study using SEM did not reveal degradation of the film structure similar to the first sample. No discontinuities formation was detected. The surface morphology is almost smooth and homogeneous, but at the same time slight waviness is observed. Figure 2, *b* shows zoomed up SEM image of the surface, which illustrates that during the polymorphic transformation when annealing or cooling is performed, the cracking of the film occurred. Apparently, this is due to the fact that during the process the film remains mechanically coupled to the substrate and does not have time to relax during recrystallization.

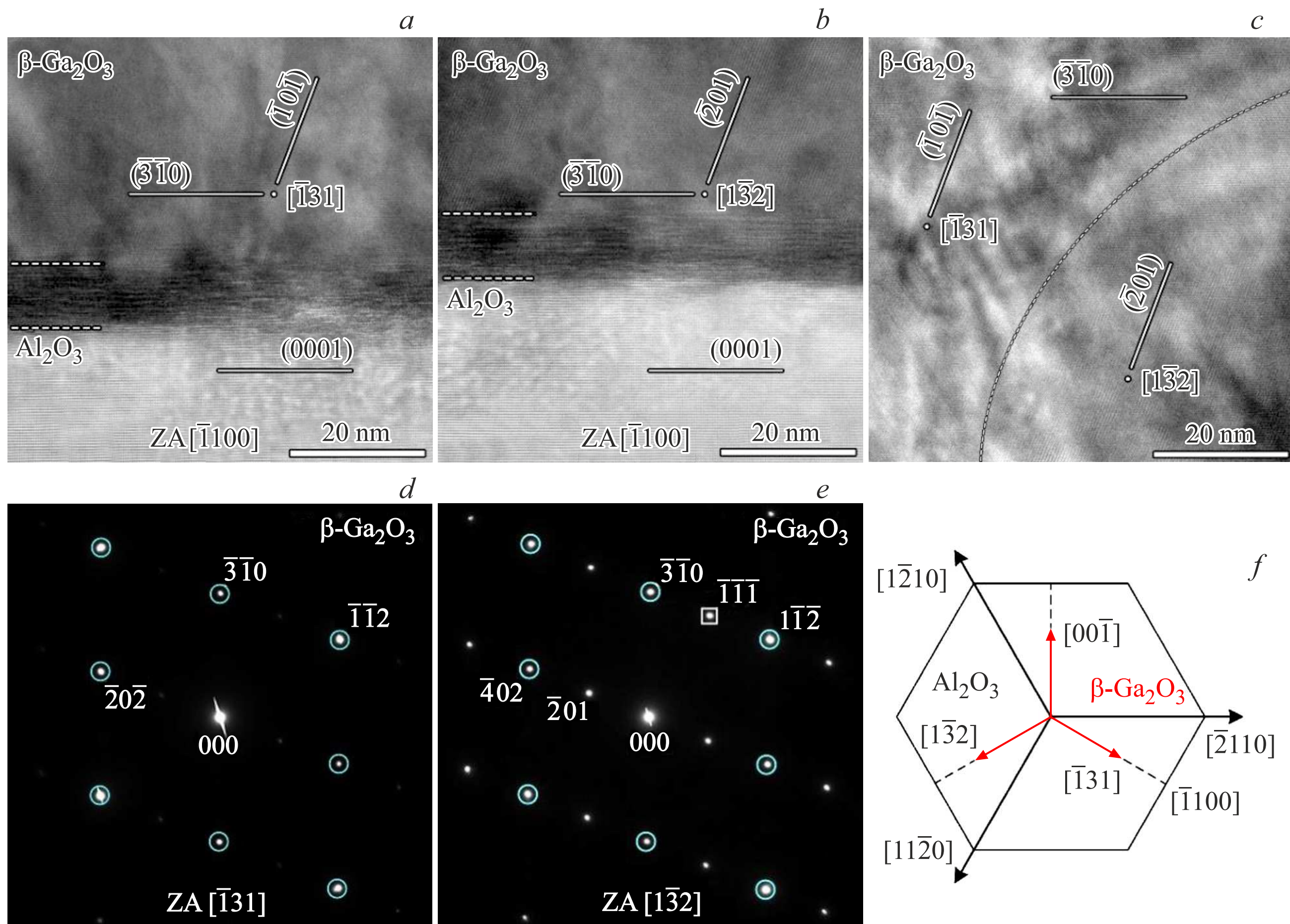


**Figure 3.** *a, b* — HREM images of region of interface with substrate for $Al_2O_3$ $[1\bar{1}00]$; *c* — HREM image of boundaries between domains; *d, e* — electron diffracton patterns corresponding to domains on images *a, b* and *c* respectively; *f* — schematic image of orientation of domains β-$Ga_2O_3$ on sapphire substrate.

The TEM image of the film cross-section in Figure 2, *c* shows that the homogeneity of its thickness changed, which correlates with the waviness observed in the SEM images. From the dark-field image of the cross section for reflection $\bar{1}\bar{1}\bar{1}$, shown in Figure 2, *d*, it is clear that the film is polycrystalline. The choice of reflection $\bar{1}\bar{1}\bar{1}$ will be explained in the further discussion of the results.

Figure 3 *a, b* shows two high-resolution TEM images (HREM) of the film-substrate interface region. In the images the substrate has the same orientation — near the zone axis $[\bar{1}100]$. HREM images of the film correspond to two different orientations of β-$Ga_2O_3$ domains. Analysis of electron microdiffraction patterns showed (see Figure 3, *d, e*) that the orientation of crystallites is characterized by one general position of the plane $(\bar{3}\bar{1}0)$ — parallel to the basal plane of the substrate. The plane $(\bar{3}10)$ can also be selected to indicate orientation. It was established that the directions $[\bar{1}31]$ and $[1\bar{3}2]$ of domains are oriented parallel to the zone axis $[\bar{1}100]$ of the substrate. This is illustrated schematically in Figure 3*f*, where it is shown that the directions $[\bar{1}31]$, $[1\bar{3}2]$ and $[00\bar{1}]$ lie in the plane $(\bar{3}\bar{1}0)$, and the angle between them is close to 120°:

$$[\bar{1}31]\widehat{\ }[00\bar{1}] = 120.2^\circ$$

$$[1\bar{3}2]\widehat{\ }[\bar{1}31] = 119.6^\circ$$

$$[00\bar{1}]\widehat{\ }[1\bar{3}2] = 120.1^\circ \qquad (1.1)$$

This corresponds to the observed results of high-temperature annealing for films κ-$Ga_2O_3$ [15], however, in our work we did not find signs of the film twinning.

Summarizing these results, one can come to a conclusion that at high temperature annealing the polymorphic transition of κ-$Ga_2O_3$ film with orientation (001) to β-$Ga_2O_3$ film consisting from domains with orientation $(\bar{3}\bar{1}0)$ occurs. The orientation relationships of domains with the substrate are as follows:

$$\beta\text{-}Ga_2O_3(\bar{3}\bar{1}0) \parallel \alpha\text{-}Al_2O_3(0001)$$

$$\beta\text{-}Ga_2O_3[\bar{1}31] \parallel \alpha\text{-}Al_2O_3\langle 1\bar{1}00\rangle$$

$$\beta\text{-}Ga_2O_3[1\bar{3}2] \parallel \alpha\text{-}Al_2O_3\langle 1\bar{1}00\rangle$$

$$\beta\text{-}Ga_2O_3[00\bar{1}] \parallel \alpha\text{-}Al_2O_3\langle 1\bar{1}00\rangle \qquad (1.2)$$

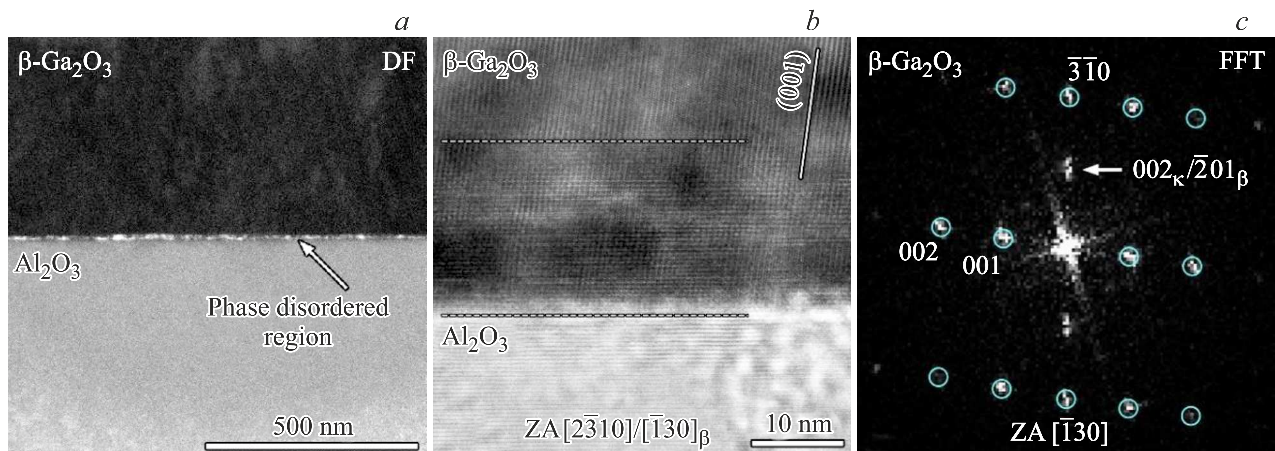


**Figure 4.** Results of study of transition region 20−30 nm above the interface. *a* — dark-field TEM image at low magnification of the transition region at the interface. The image was obtained in reflection of either 002 of $\kappa$-phase or $\bar{2}01$ of $\beta$-phase. *b* — zoomed up HREM image of this region oriented along the zone axis $[\bar{1}30]$. *c* — FFT result for the image fragment highlighted with dashed lines, confirming the presence of this order for this region. The position of the corresponding peak is indicated by an arrow.

Domain structure of $\beta$-$Ga_2O_3$ film with orientation $(\bar{3}\bar{1}0)$ can be conveniently explained with involving cubic $\gamma$-phase. When describing the structure of polymorphic modifications $Ga_2O_3$, it is effective to represent it as a set of octahedrons ($GaO_6$) and tetrahedrons ($GaO_4$) with oxygen atoms at the vertices. For $\beta$-$Ga_2O_3$the faces of tetrahedrons and octahedrons will correspond to planes of type $(\bar{2}01)$, (101), $(\bar{3}10)$, $(\bar{3}\bar{1}0)$ with a slightly distorted close-packed arrangement of oxygen atoms in them. The arrangement of oxygen layers along the normal to the plane $(\bar{2}01)$ is close to cubic 3*C* close-packed structure with alternating *ABC*. Along the normal to the plane $(\bar{3}\bar{1}0)$ $\beta$-$Ga_2O_3$ there is also a similar alternation, but with a more complex nature. In the orthorhombic $\kappa$-$Ga_2O_3$ the stacking of oxygen layers along [001] direction corresponds to 4*H* pseudohexagonal close-packed structure with alternating *ABCB*, which requires its transformation. In the cubic $\gamma$-phase there are four directions of type $\langle 111\rangle$ with *ABC* alternation, one normal to the film surface and three inclined [20,28]. Further, the difference will be in filling the octahedral and tetrahedral voids between them. Reorganization of gallium atoms in inclined planes $\{111\}$ will lead to the formation of $\beta$-$Ga_2O_3$ domains of three orientations with one common plane $(\bar{3}\bar{1}0)$, corresponding to the remaining plane (111). The choice of one orientation or another can be justified by calculation methods only, taking into account the influence of the substrate.

## 5. Boundary structure

In the electron microdiffraction patterns in Figure 3, *d, e* circles round reflections that almost completely coincide with each other for both orientations. For example, the interplanar spacing $d_{(\bar{4}02)} \approx d_{(\bar{2}0\bar{2})} \approx 2.34\,\text{Å}$ and $d_{(\bar{1}\,\bar{1}2)} = d_{(1\bar{1}\,\bar{2})} = 2.10\,\text{Å}$, and the angle between the corresponding reflections is 125.7°. For this reason, to observe domains of various orientations in dark-field TEM images, we chose the reflection $\bar{1}\bar{1}\bar{1}$, which is present for the zone axis $[1\bar{3}2]$ and absent for $[\bar{1}31]$ and $[00\bar{1}]$. On Figure 3, *e* reflection $\bar{1}\bar{1}\bar{1}$ is enclosed by square. The presence of such similarity during the transition between $[\bar{1}31]$ and $[1\bar{3}2]$ directions in the plane $(\bar{3}\bar{1}0)$ contributes to the formation of partially coherent boundaries between domains. I. e. interface along boundaries containing $[\bar{1}31]$ and $[1\bar{3}2]$ directions of adjacent domains shall not create significant stresses. At the same time, the heterogeneity of the phase contrast in Figure 3, *c* indicates that stresses are still present. The difference in orientation between regions in the image was determined using a fast Fourier transform (FFT). At the same time, such boundaries will not be formed for the direction $[00\bar{1}]$, because for this axis of zone there is no same similarity with $[1\bar{3}2]$ and $[\bar{1}31]$. No such boundaries were found during TEM study.

## 6. Transition region

In the HREM images in Figure 3 the defect region about 15−30 nm is observed near the interface, where, apparently, the polymorphic transition did not have time for complete formation. The region in the images is shown with dashed lines. This transition region, as shown in the dark-field TEM image in Figure 4, *a*, has uniform thickness and present along the entire perimeter of the interface with the substrate. The image was obtained in reflection from the second set of peaks in the X-ray pattern in Figure 2, *a*. It can be attributed to either the reflection $\bar{2}01$ of $\beta$-phase, or 002 of $\kappa$-phase, or 111 of $\gamma$-phase.

Zoomed up HREM image of this region, obtained by observation along the zone axis $[\bar{1}30]$, is shown in Figure 4, *b*. The sample was rotated in the interface plane

from the zone axis $[\bar{1}100]$ substrate zone to zone $[2\bar{3}10]$ by $\sim 19^\circ$. This corresponds to rotation from the zone axis $[\bar{1}31]$ to $[\bar{1}30]$ for the film $\beta$-$Ga_2O_3$. At this orientation the horizontal planes with large period are clearly visible in the image near the interface with the substrate, these planes disappear above the dashed boundary. Figure 4, $c$ shows the result of the Fourier transform applied to the highlighted image fragment. The transformation region does not include the sapphire substrate to avoid overlapping the peak with the forbidden reflection 0003 $\alpha$-$Al_2O_3$. The transformation clearly shows the presence of a period corresponding to the reflection either 002 of $\kappa$-phase or $\bar{2}01$ of $\beta$-phase. The peak position is indicated by the arrow. When moving along the interface, for some of the regions, this peak streaking is observed with the formation of a elongated rod. The latter indicates failures in layers stacking in this direction. Above this region this order and streaking disappear completely. To summarize, we can associate the second set of reflections observed in the X-ray pattern with the transition region located at the interface with the substrate, with thickness about 20−30 nm.

## 7. Conclusion

It is established that during annealing of $\alpha$-$Ga_2O_3$ film on sapphire substrate at temperature in the region of the beginning of the polymorphic transformation, 550−575°C, within 1 h the intense degradation of the single-crystal film occurs, accompanied by partial polymorphic transition to $\beta$-$Ga_2O_3$ phase with the formation of crystallites of new phase with a preferential orientation $(\bar{2}01)$. Degradation was localized, with the simultaneous formation of several nucleation centers and a gradual increase in their area. At the end of the specified period, for film $\sim 1.8\,\mu$m thick significant regions were observed with fragments of the original film of $\alpha$-modification that did not undergo phase transition. Thus, the study confirmed that the temperature range above 500°C is critical for technological operations with gallium oxide films of $\alpha$-modification.

During high-temperature annealing of the film $\kappa$-$Ga_2O_3$ at $T = 850^\circ$C for 30 min its structural transition to $\beta$-polymorph occurred, and new film was formed by recrystallization. According to the results of X-ray diffraction studies, it was shown that the resulting film has a mainly orientation of crystallites $(\bar{3}\,\bar{1}\,0)$. TEM study showed that rotational domains were formed with three orientations with common plane $(\bar{3}\,\bar{1}\,0)$ and with directions $[\bar{1}31]$, $[1\bar{3}2]$ and $[00\bar{1}]$ parallel to $\langle\bar{1}100\rangle$ substrate. In this case, practically coherent boundaries are formed between them, containing the directions $[\bar{1}31]$ and $[1\bar{3}2]$ of two adjacent domains, respectively.

### Funding

This work was carried out within the state assignment of Ioffe Institute of the Russian Academy of Sciences in part of thin-film growth and analyzing the results. This work was performed within the state assignment of FSRC „Crystallography and Photonics“ RAS in part of transmission electron microscopy.

### Conflict of interest

The authors declare that they have no conflict of interest.

## References

[1] T. Oshima, T. Okuno, S. Fujita. Jpn. J. Appl. Phys. Part 1 Regul. Pap. Short Notes Rev. Pap. **46**, *11*, 7217 (2007).
[2] W.S. Hwang, A. Verma, H. Peelaers, V. Protasenko, S. Rouvimov, H. (Grace) Xing, A. Seabaugh, W. Haensch, C. Van de Walle, Z. Galazka, M. Albrecht, R. Fornari, D. Jena. Appl. Phys. Lett. **104**, *20*, 203111 (2014).
[3] N.R. Taylor, M. Ji, L. Pan, P. Kandlakunta, I. Kravchenko, P. Joshi, T. Aytug, M.P. Paranthaman, L.R. Cao. Nucl. Instruments Meth. Phys. Res. Sect. A Accel. Spectrometers. Detect. Assoc. Equip. **1013**, *4*, 165664 (2021).
[4] A.V. Almaev, V.I. Nikolaev, N.N. Yakovlev, P.N. Butenko, S.I. Stepanov, A.I. Pechnikov, M.P. Scheglov, E.V. Chernikov. Sensors Actuators B **364**, 131904, (2022).
[5] J. Zhang, J. Shi, D.-C. Qi, L. Chen, K.H.L. Zhang. APL Mater. **8**, *2*, 020906, (2020).
[6] E. Ahmadi, Y. Oshima. J. Appl. Phys. **126**, *16*, 160901, (2019).
[7] V.I. Nikolaev, A.V. Chikiryaka, L.I. Guzilova, A.I. Pechnikov. PZhTF **45**, *21*, 51, (2019). (in Russian)
[8] J. Kim, D. Tahara, Y. Miura, B.G. Kim. Appl. Phys. Express **11**, *6*, (2018).
[9] M.B. Maccioni, V. Fiorentini. Appl. Phys. Express **9**, *4*, 2(2016).
[10] S. Fujita, K. Kaneko. J. Cryst. Growth **401**, 588 (2014).
[11] T. Kawaharamura, G.T. Dang, M. Furuta. Jpn. J. Appl. Phys. **51**, *4, PART 1*, 2 (2012).
[12] Y. Li, X. Xiu, W. Xu, L. Zhang, H. Zhao, Z. Xie, T. Tao, P. Chen, B. Liu, R. Zhang, Y. Zheng. Superlat. Microstruct. **152**, *2*, 106845, (2021).
[13] S.D. Lee, K. Akaiwa, S. Fujita. Phys. Status Solidi Curr. Top. Solid State Phys. **10**, *11*, 1592 (2013).
[14] I. Cora, Z. Fogarassy, R. Fornari, M. Bosi, A. Rečnik, B. Pécz. Acta Mater. **183**, 216 (2020).
[15] J. Lee, H. Kim, L. Gautam, K. He, X. Hu, V.P. Dravid, M. Razeghi. Photonics **8**, *1*, 1 (2021).
[16] R. Fornari, M. Pavesi, V. Montedoro, D. Klimm, F. Mezzadri, I. Cora, B. Pécz, F. Boschi, A. Parisini, A. Baraldi, C. Ferrari, E. Gombia, M. Bosi. Acta Mater. **140**, 411 (2017).
[17] H. Son, Y.-J. Choi, J. Hwang, D.-W. Jeon. ECS J. Solid State Sci. Technol. **8**, *7*, Q3024 (2019).
[18] R. Jinno, K. Kaneko, S. Fujita. AIP Adv. **10**, *11*, (2020).
[19] S.J. Pearton, J. Yang, P.H. Cary, F. Ren, J. Kim, M.J. Tadjer, M.A. Mastro. Appl. Phys. Rev. **5**, *1*, (2018).
[20] I. Cora, F. Mezzadri, F. Boschi, M. Bosi, M. Čaplovičová, G. Calestani, I. Dódony, B. Pécz, R. Fornari. Cryst. Eng. Commun. **19**, *11*, 1509 (2017).
[21] M. Marezio, J.P. Remeika. J. Chem. Phys. **46**, *5*, 1862 (1967).
[22] J.P. Remeika, M. Marezio. Appl. Phys. Lett. **8**, *4*, 87 (1966).

[23] J. Åhman, G. Svensson, J. Albertsson. Acta Crystallogr. C **52**, *6*, 1336 (1996).
[24] S. Yoshioka, H. Hayashi, A. Kuwabara, F. Oba, K. Matsunaga, I. Tanaka. J. Phys. Condens. Matter **19**, *34*, (2007).
[25] A.I. Pechnikov, S.I. Stepanov, A.V. Chikiryaka, M.P. Scheglov, M.A. Odnobludov, V.I. Nikolaev. Semiconductors **53**, *6*, 780 (2019).
[26] V. Gottschalch, K. Mergenthaler, G. Wagner, J. Bauer, H. Paetzelt, C. Sturm, U. Teschner. Phys. Status Solidi **206**, *2*, 243 (2009).
[27] J. Wei, K. Kim, F. Liu, P. Wang, X. Zheng, Z. Chen, D. Wang, A. Imran, X. Rong, X. Yang, F. Xu, J. Yang, B. Shen, X. Wang. J. Semiconductors **40**, *1*, 012802 (2019).
[28] N. Husnain, E. Wang, S. Fareed, M.T. Anwar. Catalysts **9**, *12*, (2019).

*Translated by I.Mazurov*